

## AN UNLOADING AND RELOADING STRESS-STRAIN MODEL FOR CONCRETE CONFINED BY TIE REINFORCEMENTS

Junichi SAKAI<sup>1</sup> And Kazuhiko KAWASHIMA<sup>2</sup>

### SUMMARY

This paper presents a series of uniaxial compressive loading tests on concrete cylinder confined by tie reinforcements in order to develop an unloading and reloading stress-strain model. The specimens were 600mm high and 200mm in diameter with various volumetric ratios of tie reinforcement and cylinder strengths of concrete. The tie reinforcement ratio  $\rho_s$  and the cylinder strength of concrete  $\sigma_{c0}$  were varied from 0.67% to 2.67% and from 23.0MPa to 36.7MPa, respectively. The number of unloading from an unloading strain and reloading was studied as one of the parameters.

It is found from the test results that unloading and reloading do not essentially change the shape of envelope curves of stress-strain relation, and that to predict an unloading and reloading paths, the plastic strain  $\varepsilon_{pl-n}$  and the stress at the unloading strain  $\sigma_{ul-n}$  are controlling parameters. These controlling parameters were analysed based on the test data to propose an empirical relation. Unloading path was idealized as a parabolic function, while reloading path was idealized as a combination of a parabolic curve and a straight line. The proposed unloading and reloading stress-strain model was compared to the test results. The comparison showed that the predicted unloading and reloading stress-strain relation provides good agreement with the test data.

### INTRODUCTION

To evaluate seismic performance of reinforced concrete bridge piers, it is important to provide an appropriate stress-strain model of concrete confined by tie reinforcements. Various studies have been conducted on the confinement effect based on uniaxial loading [Sheikh and Uzumeri, 1980, Sheikh and Uzumeri, 1982, Mander et al., 1988a, Mander et al., 1988b, Hoshikuma et al., 1997]. Although various models are available for stress-strain relations of confined concrete under monotonic loading, few studies are available for unloading and reloading hysteresses.

Sinha et al. [1964] and Karsan et al. [1969] conducted uniaxial compression tests on unconfined concrete specimens to evaluate the unloading and reloading paths. Park et al. [1972], Ristic [1988] and Mander et al. [1988a, 1988b] proposed stress-strain models of confined concrete including an unloading and reloading paths. Park et al. idealized both unloading and reloading paths to be straight lines. Ristic proposed a parabolic unloading path and a straight reloading path. The plastic strain, which corresponds to the strain where stress becomes 0 on an unloading path, was proposed 50% of the strain at an unloading point. Mander et al. proposed a fractional expression to the unloading path and a straight line to the reloading path. To predict the plastic strain, Mander et al. assumed an unloading secant modulus, taking into account the confinement effect by tie reinforcement. Although the above stress-strain models have been widely used for seismic analyses of structures, they did not study the effect of cyclic unloading and reloading.

In this research, a series of uniaxial compressive loading tests on confined concrete were conducted to develop an unloading/ reloading hysteresses when unloading and reloading are repeated.

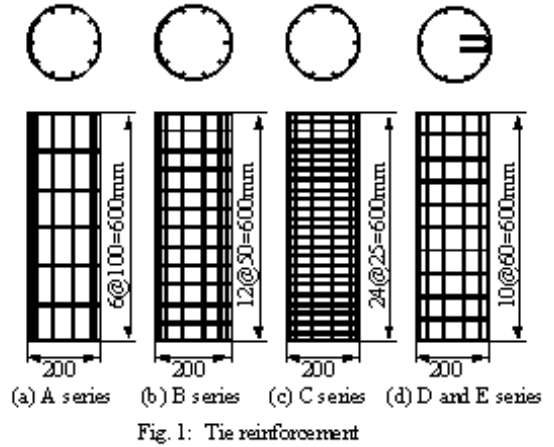
<sup>1</sup> Dept of Civil Engineering, Tokyo Institute of Technology, , Japan, Email: sjun@cv.titech.ac.jp

<sup>2</sup> Dept of Civil Engineering, Tokyo Institute of Technology, , Japan, Email: kawasima@cv.titech.ac.jp

## TEST SPECIMENS AND LOADING HYSTERESES

**Table 1: Test series**

Test series	Cylinder strength of concrete $\sigma_{c0}$ (MPa)	Tie reinforcement	
		Spacing $s$ (mm)	Volumetric ratio $\rho_s$ (%)
A	23.0	100	0.67
B		50	1.33
C		25	2.67
D	36.7	60	1.14
E	29.8		



The test series are described in Table 1. The specimens were 600mm high and 200mm in diameter. Five series of tests with 4 specimens each were conducted changing the volumetric ratio of tie reinforcement  $\rho_s$  and cylinder strength of concrete  $\sigma_{c0}$  as parameters. The arrangements of tie reinforcements are shown in Fig. 1. To evaluate the confinement effect, the tie reinforcement ratio  $\rho_s$  was 0.67% (A series), 1.33% (B series) and 2.67% (C series) with a constant cylinder strength  $\sigma_{c0}=23.0\text{MPa}$ . On the other hand, in order to study the effect of cylinder strength of concrete with a constant tie reinforcement ratio  $\rho_s=1.14\%$ , two cylinder strengths of concrete were considered; 37.6MPa (D series) and 29.8MPa (E series). 6mm deformed reinforcements with yield strength of 380MPa were used for the tie reinforcements. A total of 10 deformed bars with 10mm diameter (A, B and C series) and 6mm diameter (D and E series) were provided in each specimen for the longitudinal reinforcements.

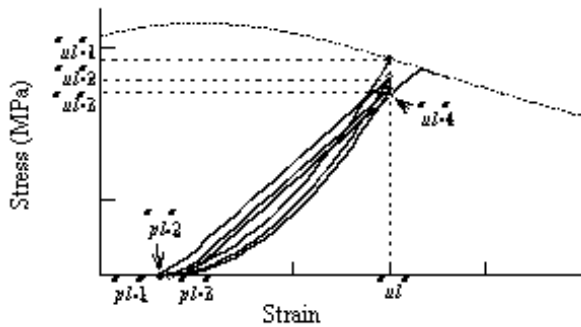


Fig. 2: Stress-strain relation at unloading and reloading paths

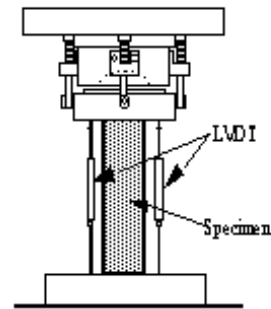


Fig. 3: Test setup

A typical unloading and reloading stress-strain relation is shown in Fig. 2. To develop an unloading/ reloading path model, two parameters; plastic strain  $\epsilon_{pl-n}$  and stress  $\sigma_{ul-n}$ , have to be determined. The plastic strain  $\epsilon_{pl-n}$  is the strain where stress becomes 0 on the  $n$ -th path unloaded from  $\epsilon_{ul}$ . The stress  $\sigma_{ul-n+1}$  is the stress reached at  $\epsilon_{ul}$  after  $n$ -th reloading from the plastic strain  $\epsilon_{pl-n}$ .

The unloading strain  $\epsilon_{ul}$  was varied in the range  $0 \leq \epsilon_{ul} \leq 0.03$  as

$$\epsilon_{ul} = \frac{k}{4} \epsilon_{cc} \quad (k = 1, 2, \dots, m) \tag{1}$$

where  $\epsilon_{cc}$  = strain at peak stress and  $m$  = the number of  $\epsilon_{ul}$  where unloaded (number of unloading points).

Fig. 3 shows the experimental setup. The specimens were subjected to uniaxial compressive loading under displacement control. The axial force was measured by a load cell. Axial stress was calculated by dividing the measured axial load by an initial area of a specimen. Axial deformation of the specimen was measured by two

LVDTs placed on opposite sides of the specimen. Axial strain was calculated by dividing the relative displacement measured between top and bottom surfaces by an initial height of a specimen.

## A STRESS-STRAIN RELATION FOR UNLOADING AND RELOADING

### 3.1 Effect of Unloading and Reloading on Envelope Curve

Fig. 4 shows stress-strain curves of a specimen with  $\rho_s = 0.67\%$  (A series) subjected to a monotonic loading and an unloading/ reloading. The number of unloading points  $m$  was 5 for A-2 and 10 for A-3, and a single unloading/ reloading was conducted at each loading test. As shown in Fig. 5, the envelopes of stress-strain of the specimens subjected to unloading and reloading are close to that of the specimens subjected to monotonic loading.

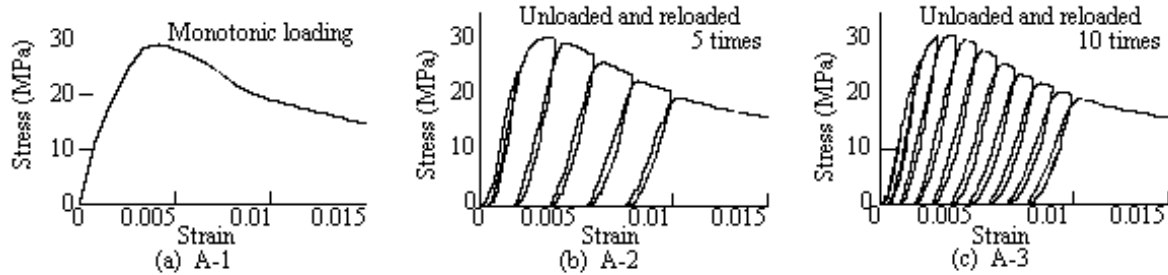


Fig. 4: Stress-strain relation ( $\sigma_{c0}=23.0\text{MPa}$ ,  $\rho_s=0.67\%$ )

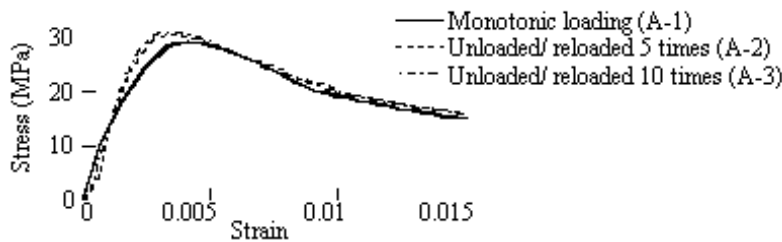


Fig. 5: Effect of  $m$  on envelope curve

### 3.2 Effect of Tie Reinforcement Ratio and Cylinder Strength of Concrete

Fig. 6 shows the effect of tie reinforcement ratios  $\rho_s$  on unloading and reloading paths. The plastic strain  $\epsilon_{pl,1}$  is in the range of 0.0032~0.0036 and is almost independent of the tie reinforcement ratio  $\rho_s$ . On the other hand, the stress reached at the unloading strain  $\epsilon_{ul}$  on the reloading path ( $\sigma_{ul,2}$ ) is smaller than the original stress at

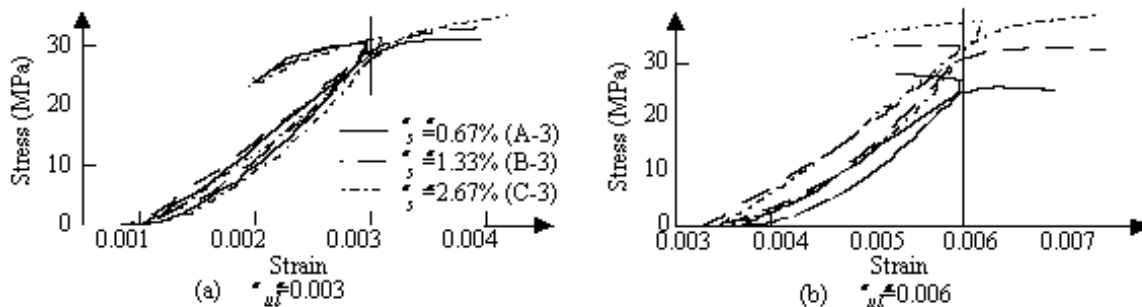


Fig. 6: Effect of tie reinforcement ratio  $\rho_s$

the first unloading ( $\sigma_{ul,1}$ ). To evaluate the deterioration of stress at  $\epsilon_{ul}$  after unloading and reloading, a stress deterioration ratio  $\beta_n$  is defined as

$$\beta_n = \frac{\sigma_{ul,n+1}}{\sigma_{ul,n}} \quad (2)$$

The stress deterioration ratio  $\beta_1$  is 0.914~0.919 in Fig. 6.

To show the effect of cylinder strength of concrete  $\sigma_{c0}$  on the unloading and reloading paths, unloading and reloading paths of concrete with  $\sigma_{c0}=36.7\text{MPa}$  and  $29.8\text{MPa}$ , when unloaded from  $\varepsilon_{ul}=0.003$  and  $0.006$ , are compared in Fig. 7. On the unloading and reloading paths when unloaded from  $\varepsilon_{ul}=0.003$ ,  $\sigma_{ul-1}$  of the specimen with  $\sigma_{c0}=36.7\text{MPa}$  is larger than that of the specimen with  $\sigma_{c0}=29.8\text{MPa}$ . However  $\varepsilon_{pl-1}$  is about  $0.001$  and the stress deterioration ratios  $\beta_1$  is about  $0.95$ . It is noteworthy that the plastic strain  $\varepsilon_{pl-1}$  and the stress deterioration ratio  $\beta_1$  are less significantly affected by  $\rho_s$  and  $\sigma_{c0}$ .

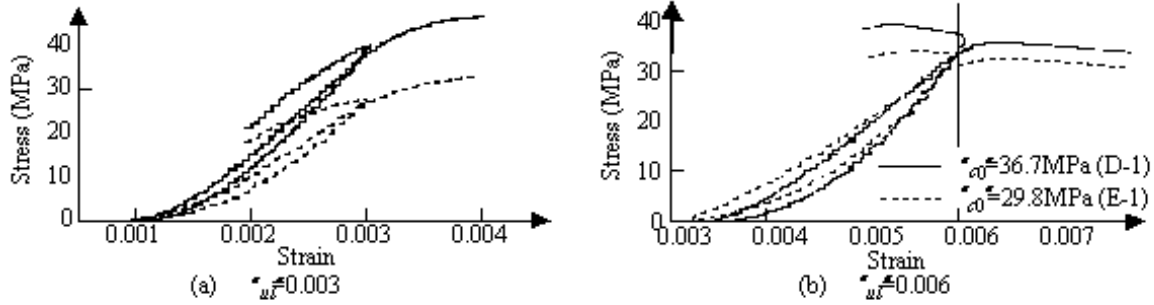


Fig. 7: Effect of cylinder strength of concrete  $\sigma_{c0}$

### 3.3 Effect of Repetition of Unloading and Reloading

Fig. 8 shows the stress-strain relation of a specimen subjected to unloading and reloading 3 times each. A monotonic loading curve (A-1) is also presented here for comparison. Similar to Fig. 5, the envelope of stress-strain of the specimen subjected to unloading/ reloading 3 times each is close to that of the specimen subjected to the monotonic loading. Fig. 9 shows the stress vs. strain of the E-2 Specimen unloaded from  $\varepsilon_{ul}=0.005$  and reloaded 10 times. When it was first unloaded from  $\varepsilon_{ul}=0.005$ , the initial stress at unloading point  $\sigma_{ul-1}$  was  $35.1\text{MPa}$ . It then decreased along the unloading path, and the first plastic strain  $\varepsilon_{pl-1}$  was  $0.00228$ . After unloaded and reloaded 10 times, the plastic strain  $\varepsilon_{pl-10}$  increased to  $0.00262$  while the unloading stress  $\sigma_{ul-11}$  decreased to  $26.2\text{MPa}$ . Hence,  $\sigma_{ul-n}$  decreases and  $\varepsilon_{pl-n}$  increases as the number of unloading and reloading  $n$  increases.

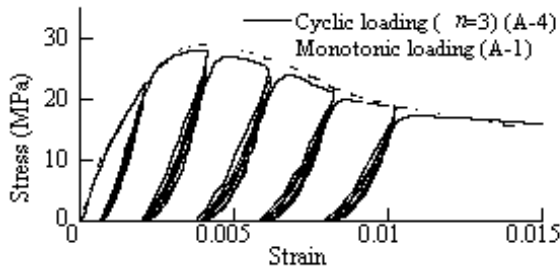


Fig. 8: Stress-strain relation under unloading and reloading 3 times each

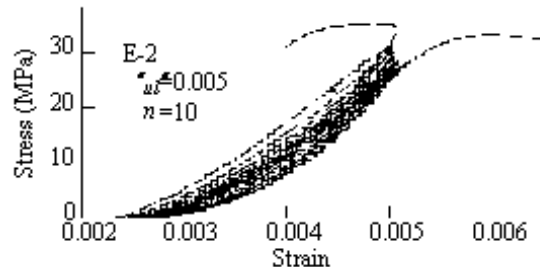


Fig. 9: Hysteresis under unloading and reloading 10 times

## MODELING OF UNLOADING AND RELOADING PATH

To evaluate the unloading and reloading paths, the normalized stress  $\tilde{\sigma}$  and the normalized strain  $\tilde{\varepsilon}$  are defined as

$$\tilde{\sigma} = \frac{\sigma_c}{\sigma_{ul-n}}; \quad \tilde{\varepsilon} = \frac{\varepsilon_c - \varepsilon_{pl-n}}{\varepsilon_{ul} - \varepsilon_{pl-n}} \quad (3)$$

Fig. 10 shows  $\tilde{\sigma}$  vs.  $\tilde{\varepsilon}$  relations which were presented in Figs. 6 and 7. A predicted relation, which will be described later, is also presented for comparison in Fig. 10. It is noted that the effect of  $\rho_s$  and  $\sigma_{c0}$  is insignificant on  $\tilde{\sigma}$  vs.  $\tilde{\varepsilon}$  relation. They are thus represented as

$$\text{Unloading Path:} \quad \sigma_c = \sigma_{ul-n} \left( \frac{\varepsilon_c - \varepsilon_{pl-n}}{\varepsilon_{ul} - \varepsilon_{pl-n}} \right)^2 \quad (4)$$

$$\text{Reloading Path: } \sigma_c = \begin{cases} 2.5\sigma_{ul \cdot n} \left( \frac{\varepsilon_c - \varepsilon_{pl \cdot n}}{\varepsilon_{ul} - \varepsilon_{pl \cdot n}} \right)^2 & 0 \leq \tilde{\varepsilon} < 0.2 \\ E_{rl}(\varepsilon_c - \varepsilon_{ul}) + \sigma_{ul \cdot n+1} & 0.2 \leq \tilde{\varepsilon} \leq 1.0 \end{cases} \quad (5)$$

where  $E_{rl}$  is the averaged modulus of the reloading, and is given as

$$E_{rl} = \frac{\sigma_{ul \cdot n+1} - 0.1\sigma_{ul \cdot n}}{0.8(\varepsilon_{ul} - \varepsilon_{pl \cdot n})} \quad (6)$$

$\tilde{\sigma}$  vs.  $\tilde{\varepsilon}$  relation obtained from Eqs. (4) and (5) is presented in Fig. 10. The predicted unloading and reloading paths provide good agreement with the test results.

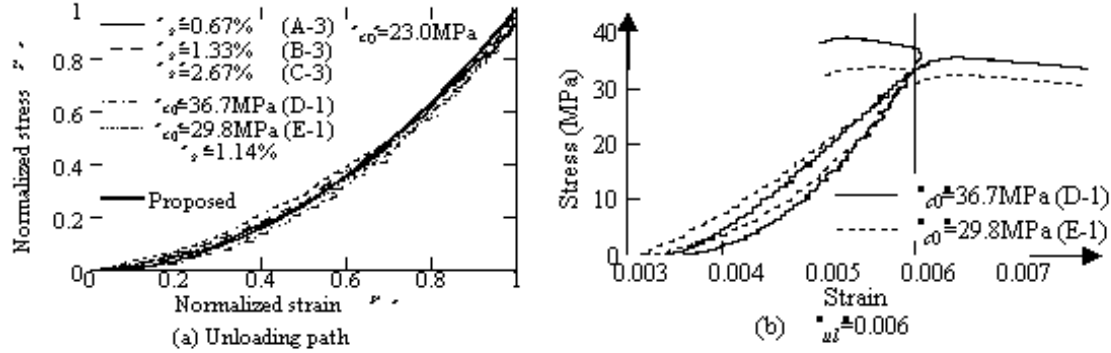


Fig. 10: Normalized stress  $\tilde{\sigma}$  vs. normalized stress  $\tilde{\varepsilon}$  relations

#### EVALUATION OF PARAMETERS OF UNLOADING AND RELOADING PATHS

In Eqs. (4) and (5), the plastic strain  $\varepsilon_{pl \cdot n}$  and the stress at unloading strain  $\sigma_{ul \cdot n}$  are required to evaluate the unloading/ reloading paths. As shown in Figs. 6 and 7, when it was unloaded from  $\varepsilon_{ul} = 0.003$  or  $0.006$ , the plastic strain  $\varepsilon_{pl \cdot 1}$  and  $\beta_1$  were almost independent of  $\rho_s$  or  $\sigma_{c0}$ . Fig. 11 shows how  $\beta_n$  changes when it was unloaded at other  $\varepsilon_{ul}$ . Since other cases show the similar variation,  $\beta_n$  for  $n=1$  and  $5$  is presented here. It can be seen that  $\beta_1$  and  $\beta_5$  are almost constant in the range  $0.0035 \leq \varepsilon_{ul} \leq 0.03$ . Fig. 12 shows how  $\beta_n$  averaged in this range varies in accordance with  $n$ . The stress deterioration ratio  $\beta_n$  is thus represented as

$$1 \leq n \leq 2: \quad \beta_n = \begin{cases} 1 & 0 \leq \varepsilon_{ul} \leq 0.001 \\ 1 - (10n - 22)(\varepsilon_{ul} - 0.001) & 0.001 < \varepsilon_{ul} < 0.0035 \\ 0.920 + 0.025(n - 1) & 0.0035 \leq \varepsilon_{ul} \leq 0.03 \end{cases} \quad (7)$$

$$n \geq 3: \quad \beta_n = \begin{cases} 1 & 0 \leq \varepsilon_{ul} \leq 0.001 \\ 1 - (2n + 8)(\varepsilon_{ul} - 0.001) & 0.001 < \varepsilon_{ul} < 0.0035 \\ 0.965 + 0.005(n - 3) & 0.0035 \leq \varepsilon_{ul} \leq 0.03 \end{cases} \quad (8)$$

where  $\beta_n \leq 1$ .

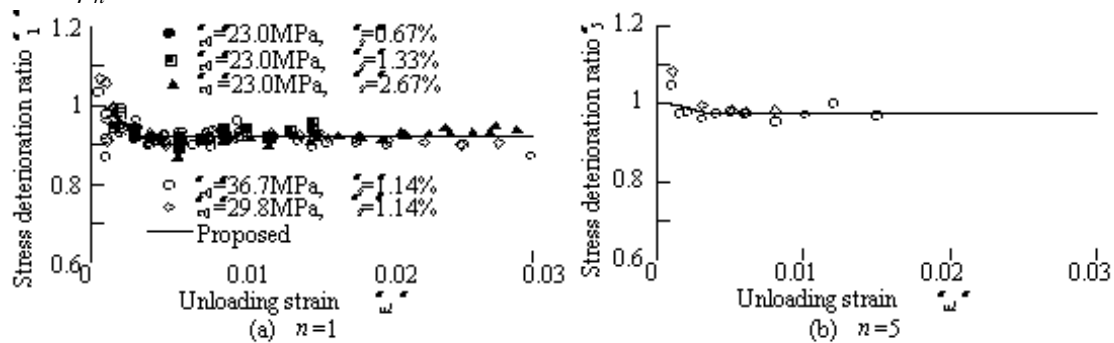


Fig. 11: Stress deterioration ratio  $\beta_n$  and unloading strain  $\varepsilon_{ul}$  relation

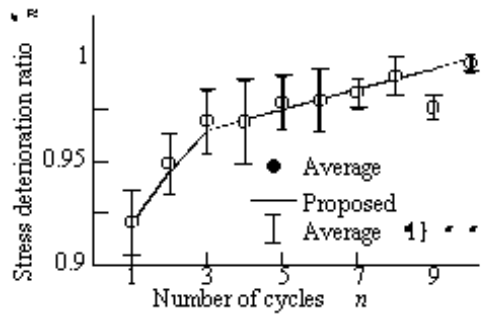


Fig. 12: Dependence of stress deterioration ratio on number of cycles  $n$

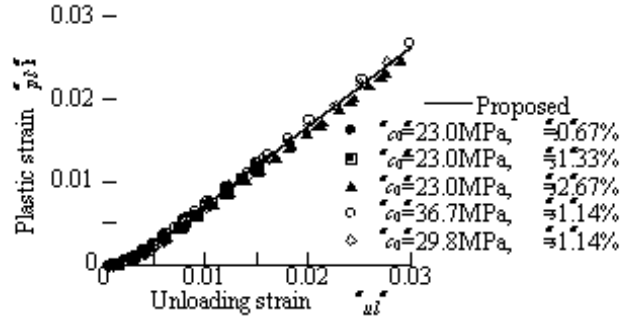


Fig. 13: Unloading strain relation

Fig. 13 shows the relation between  $\epsilon_{ul}$  and  $\epsilon_{pl.1}$ . It is represented as

$$\epsilon_{pl.1} = \begin{cases} 0 & 0 \leq \epsilon_{ul} \leq 0.001 \\ 0.40(\epsilon_{ul} - 0.001) & 0.001 < \epsilon_{ul} < 0.0035 \\ 0.96(\epsilon_{ul} - 0.00245) & 0.0035 \leq \epsilon_{ul} \leq 0.03 \end{cases} \quad (9)$$

To evaluate the increasing of the plastic strain  $\epsilon_{pl.n}$  after reloaded from  $\epsilon_{pl.n-1}$  and unloaded at the same unloading strain  $\epsilon_{ul}$ , an increasing ratio of the plastic strain  $\gamma_n$  is defined as

$$\gamma_n = \frac{\epsilon_{ul} - \epsilon_{pl.n}}{\epsilon_{ul} - \epsilon_{pl.n-1}} \quad (10)$$

Fig. 14 shows  $\epsilon_{ul}$  vs.  $\gamma_n$  relation for  $n=2$  and 5. Since  $\gamma_2$  and  $\gamma_5$  are almost constant in the range of  $0 \leq \epsilon_{ul} \leq 0.03$ ,  $\gamma_n$  averaged in this range vs. the number of unloading and reloading  $n$  is shown in Fig. 15. It is represented as

$$\gamma_n = \begin{cases} 0.945 & n = 2 \\ 0.965 + 0.005(n - 3) & n \geq 3 \end{cases} \quad (11)$$

where  $\gamma_n \leq 1$ .

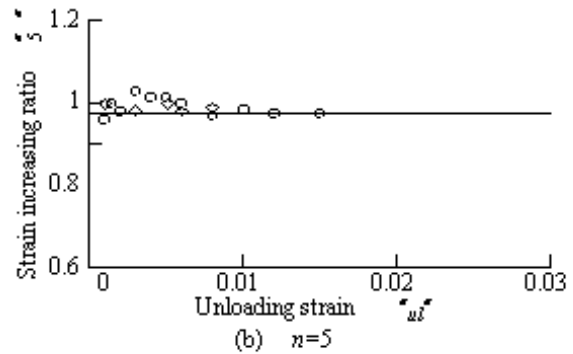
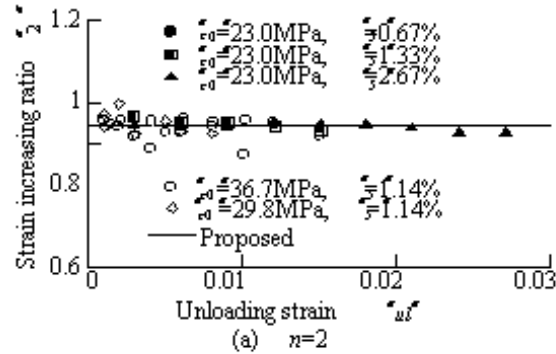


Fig. 14: Strain increasing ratio  $\gamma_n$  and unloading strain  $\epsilon_{ul}$  relation

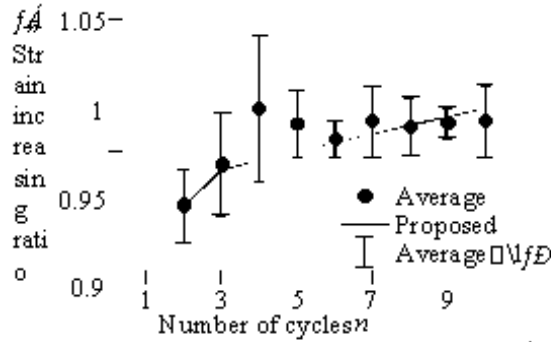


Fig. 15: Dependence of strain increasing ratio of  $A_n$  on number of cycles  $n$

### EVALUATION OF THE PROPOSED MODEL

Based on Eq. (9), the plastic strain  $\varepsilon_{pl,1}$  after the first unloading from  $\varepsilon_{ul}$  is obtained. When unloading was repeated, the plastic strain  $\varepsilon_{pl,n}$  is determined from Eqs. (10) and (11). Substituting  $\varepsilon_{pl,n}$  into Eq. (4), one obtains the unloading path. On the other hand, in evaluating the reloading path,  $\beta_n$  in Eq. (2) needs to be determined first from Eqs. (7) and (8). Substituting  $\sigma_{ul,n}$  into Eq. (5), one obtains the reloading path.

To confirm the effectiveness of the proposed model, stress-strain hystereses of unloading and reloading paths between the analysis and the experiment are compared for A-2 and B-2 as shown in Fig. 16. It should be noted here that only unloading and reloading paths are presented in the proposed hystereses. It was assumed that the unloading in the analyses starts from the strains where unloaded in the experiment and that the reloading path

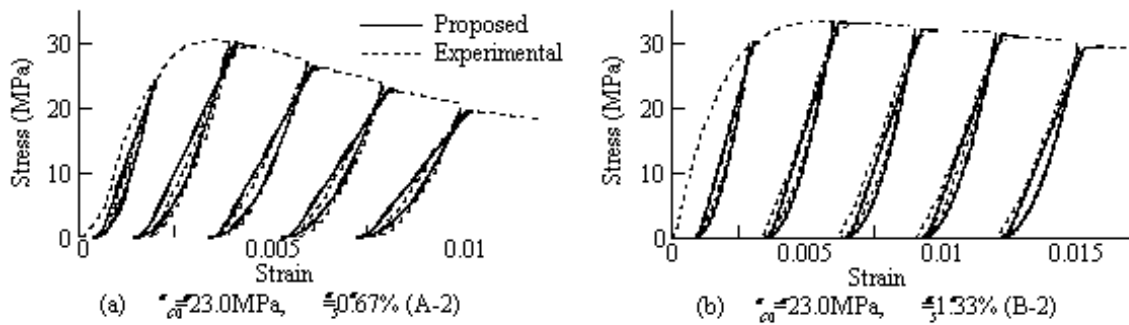


Fig. 16: Proposed vs. experimental stress-strain relations at unloading and reloading paths

builds up in the analyses until it intersects the envelope obtained from the experiment. The predicted stress-strain relation represents the behavior of the test results. It is noteworthy that  $\varepsilon_{pl,1}$  and  $\sigma_{ul,2}$  agreed quite well with the test result. Fig. 17 compares a stress-strain relation of the specimen E-2 under unloading and reloading 10 times. It can be also said that the proposed results provide good agreement.

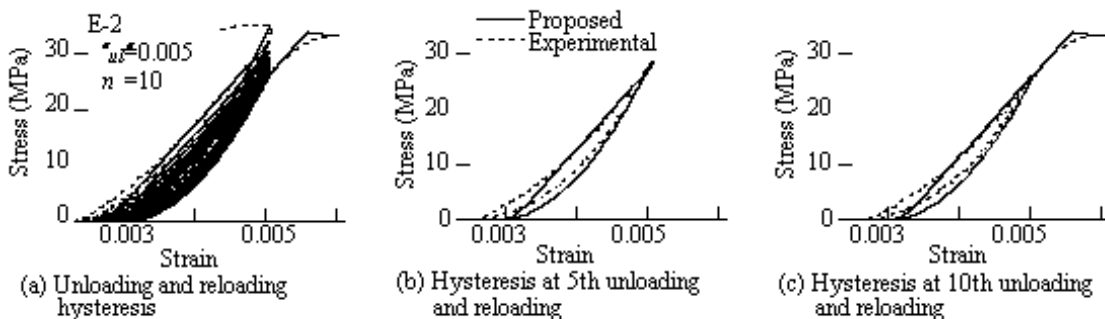


Fig. 17: Proposed vs. experimental stress-strain hystereses unloaded and reloaded 10 times

## CONCLUSIONS

To develop an unloading and reloading stress-strain model for concrete confined by tie reinforcements, a series of uniaxial compression test were conducted. Based on the tests presented herein, the following conclusions may be deduced:

1. The effect of unloading and reloading on the stress-strain envelope curve is less significant.
2. The plastic strain  $\varepsilon_{pl,1}$  and the stress deterioration ratio  $\beta_1$  of the specimens unloaded at the same strain  $\varepsilon_{ul}$  are less dependent on the tie reinforcement ratio  $\rho_s$  or cylinder strength of concrete  $\sigma_{c0}$ . Eqs. (7) and (9) provide reasonable evaluation of  $\varepsilon_{pl,1}$  for an unloading path and  $\beta_1$  for a reloading path.
3.  $\sigma_{ul,n}$  decreases and  $\varepsilon_{pl,n}$  increases as the number of unloading and reloading  $n$  increases. To evaluate  $\sigma_{ul,n}$  and  $\varepsilon_{pl,n}$ , Eqs. (7), (8) and (11) are proposed.
4. The proposed stress-strain model provides a good agreement with the unloading and reloading stress-strain relation.

## REFERENCES

- Hoshikuma, J., Kawashima, K., Nagaya, K. and Taylor, A. W. (1997), "Stress-strain model for confined reinforced concrete in bridge piers," *J. Struct. Engrg., ASCE*, Vol. 123, No. 5, pp. 624-633
- Karsan, I. D. and Jirsa, J. O. (1969), "Behavior of concrete under compressive loadings," *J. Struct. Div., ASCE*, Vol. 95, No. ST12, pp. 2543-2563
- Mander, J. B., Priestley, M. J. N. and Park, R. (1988a), "Observed stress-strain behavior of confined concrete," *J. Struct. Engrg., ASCE*, Vol. 114 No. 8, pp. 1827-1849
- Mander, J. B., Priestley, M. J. N. and Park, R. (1988b), "Theoretical stress-strain model for confined concrete," *J. Struct. Engrg., ASCE*, Vol. 114, No. 8, pp. 1804-1826
- Park, R., Kent, D. C. and Sampson, R. A. (1972), "Reinforced concrete member with cyclic loading," *J. Struct. Div., ASCE*, Vol. 98, No. 7, pp. 1341-1360
- Ristic, D. (1988), "Nonlinear behavior and stress-strain based modeling of reinforced concrete structure under earthquake induced bending and varying axial loads," School of Engineering, Kyoto University, Kyoto, Japan
- Sheikh, S. A. and Uzumeri, S. M. (1980), "Strength and ductility of tied concrete columns," *J. Struct. Div., ASCE*, Vol. 106, No. ST5, pp. 1079-1102
- Sheikh, S. A. and Uzumeri, S. M. (1982), "Analytical model for concrete confinement in tied columns," *J. Struct. Div., ASCE*, Vol. 108, No. ST12, pp. 2703-2722, 1982
- Sinha, B. P., Gerstle, K. H., and Tulin, L. G. (1964), "Stress-strain relations for concrete under cyclic loading," *Am. Concr. Inst. J.*, Vol. 61, No. 2, pp. 195-211